Exploring the Effect of Surface Machining Treatments on Microstructure of Cold-Rolled 316L Austenitic Stainless Steel and Alloy 182

L. Volpe[1], M.G. Burke[1], Q. Zaiqing[2], U. Ehrnstén[2], A. Treichel[3], S. Ritter[3], A. Hojna[4], M. Herbst[5], R. Kilian[5], A. Maurotto[6], M. Vankeerberghen[7], A. Dinu[8], C. Rainasse[9], R. Novotný[10], B. Zajec[11], M. Chatterton[12], V. Slugen[13], I. Kurt[14], F. J. Perosanz[15]

[1]Materials Performance Centre, University of Manchester, UK, liberato.volpe@manchester.ac.uk
[2]VTT Technical Research Centre of Finland Ltd., Espoo, Finland, [3]Paul Scherrer Institute (PSI), Villigen, Switzerland, [4]CVR, UJV Group, Rez, Czech Republic, [5]Framatome GmbH, Erlangen, Germany, [6]NAMRC, University of Sheffield, UK, [7]SCK•CEN, Mol, Belgium, [8]RATEN ICN, Pitesti, Romania, [9]EdF, Les Renardières, France, [10]EC JRC, Petten, The Netherlands, [11]ZAG, Ljubljana, Slovenia, [12]Jacobs, Warrington, UK, [13]STUBA, Bratislava, Slovak Republic, [14]ENSA, Maliaño, Spain, [15]CIEMAT, Madrid, Spain

Background

Material microstructure has an important effect on environment-sensitive performance of structural alloys during the initiation stages and early growth of environmentally-assisted cracks (EAC) [1,2]. The near-surface microstructural proprieties of an alloy can be strongly affected by industrial surface machining operations [3]. However, there is no systematic study of the machining effect on the EAC initiation due to the complex relationship between alloy/microstructure, local surface deformation, environment and the long time needed to perform the EAC experiments under appropriate light water reactor (LWR) conditions. Thus, the Horizon 2020 MEACTOS program is addressing this important issue to develop optimized processing for improved EAC performance for LWR. More information can be found at https://meactos.eu/documents/.

In this wok, the effect of different industrial surface machining treatments on the near-surface microstructure of cold-worked (by rolling) 316L austenitic stainless steel (CW 316L SS) and Ni-base Alloy 182 (A182) were examined using advanced characterisation techniques. The different machining processes induced the formation of an ultrafine-grained (UFG) and deformed layers beneath the surface. These microstructural changes may affect the initiation and propagation of EAC cracking.

Experimental Approach

The surfaces of interest (T-L plane) of dog-bone tapered samples of CW 316L SS and A182 were prepared with a variety of different surface machining processes including: 1) a baseline reference surface (RS) prepared with an ISO/FEPA P2000 grinding paper; 2) standard treatment industrial (STI); 3) surface advanced machining (SAM); and 5) shot peening (SP) (for A182 only).

Field emission gun scanning electron microscopy (FEG-SEM - Zeiss Merlin equipped with an Oxford Instruments Xmax Extreme 100 windowless SDD Energy Dispersive X-Ray (EDX) spectrometer and Aztec analysis system), focused ion beam (FIB) microscopy (FEI Helios NanoLab 660) and transmission electron microscopy (TEM) (FEI LaB_6 T20 operated at 200 kV) were used to characterize the samples prior to the EAC experiments. SEM evaluations used both secondary electron (SE) and backscattered electron (BSE) imaging modes to analyse the surface and the near-surface regions of the specimens. Transmission Kikuchi diffraction (TKD), bright-field (BF) TEM imaging coupled with selected area electron diffraction (SAD) were used to analyze the UFG layer.

Results

Cold Rolled 316L Stainless Steel

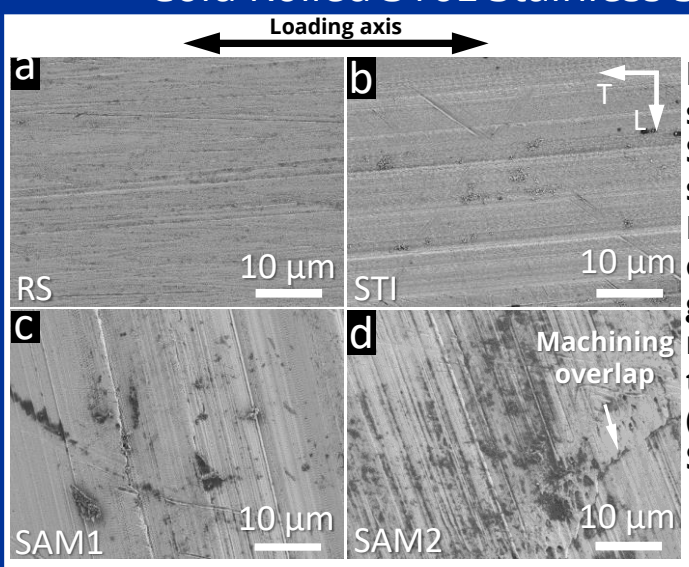

Fig.1: SE images of the surfaces of the CW316L SS with the different surface processes. Note the different orientations of the grinding / machining marks with respect to the loading axis: (a) RS; (b) STI; (c) SAM1 and (d) SAM2.

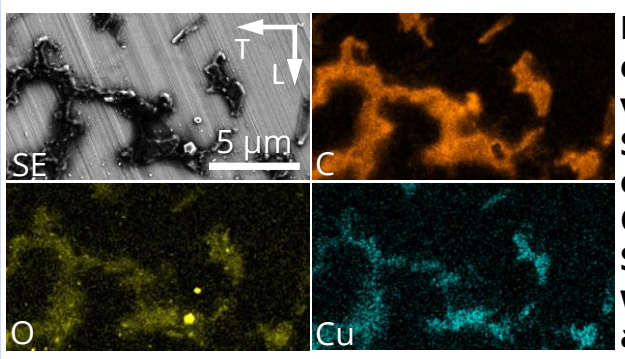

Fig.2: EDX elemental maps extracted from the low voltage FEGSEM-EDX Spectrum Image dataset obtained from the SAM2 CW316L SS specimen. Significant deposits of Cu/O were observed that may affect the EAC behavior.

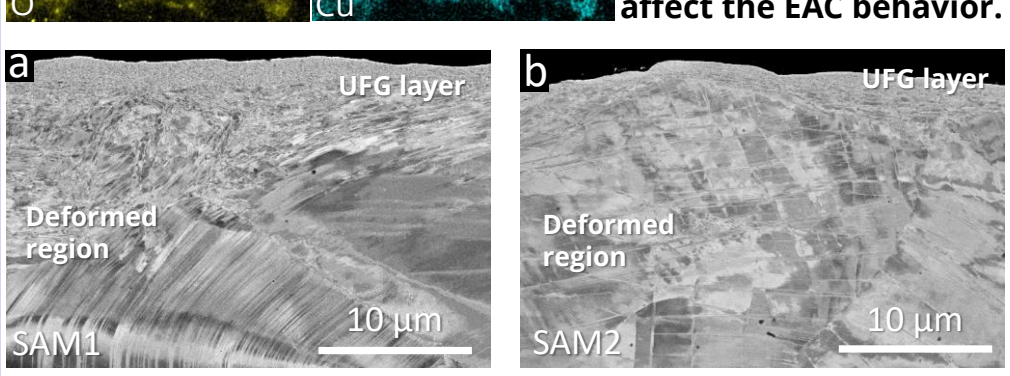

Fig.3: BSE images of cross-section samples showing the near-surface microstructure of CW316L SS machined with (a) SAM1 and (b) SAM2 surface conditions (T-S plane).

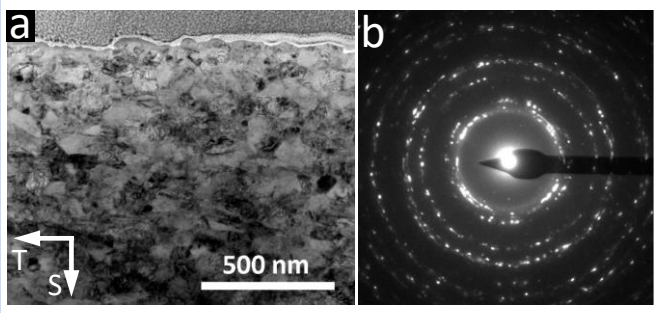

Fig.4: (a) BF-TEM image showing the UFG layer in the near-surface region (T-S plane) of SAM2 CW 316L SS, confirmed by the discrete rings visible in the (b) SADP.

As-Deposited Alloy 182

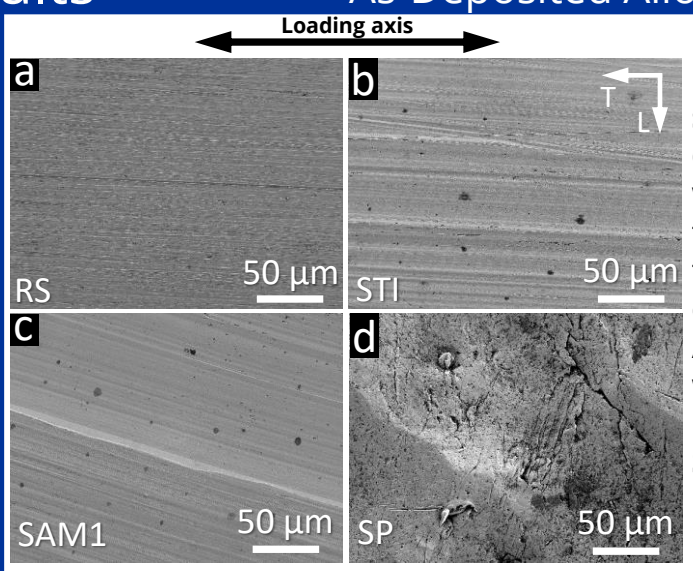

Fig.5: SE images of the surfaces of the A182 deposits (simulated weld structure) with the different surface treatments. Note the orientation of grinding / machining marks with respect to the loading axis: (a) RS; (b) STI; (c) SAM1 and (d) SP.

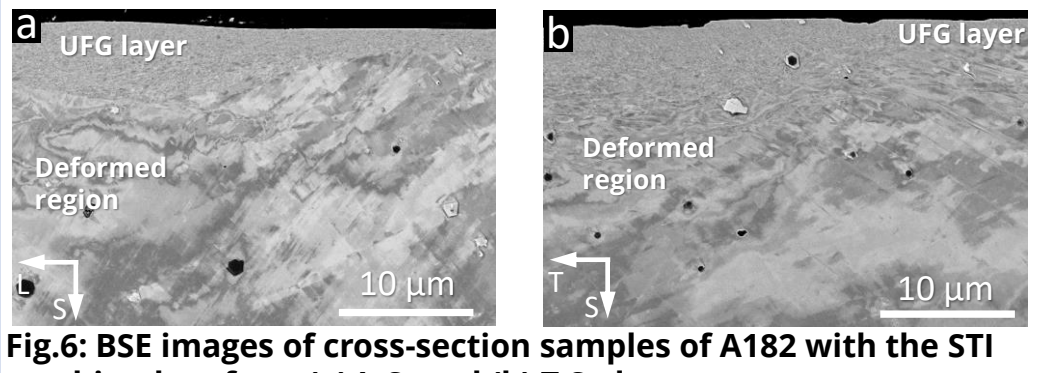

Fig.6: BSE images of cross-section samples of A182 with the STI machined surface: (a) L-S, and (b) T-S planes.

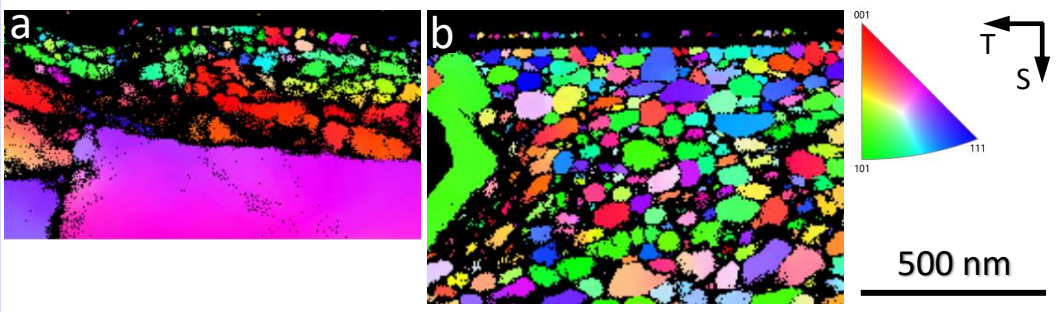

Fig.7: TKD analyses of UFG layer for the A182 for the (a) RS and (b) STI surfaces. Note the random orientation of the nanograins and the different UFG layer depth of the (a) RS and (b) STI surfaces.

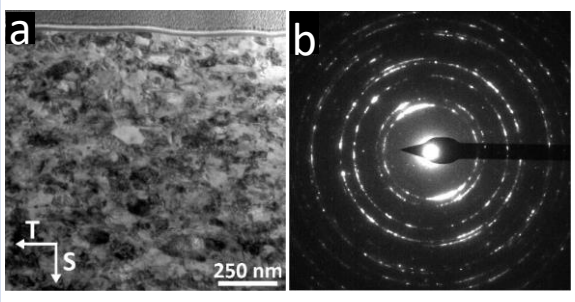

Fig.8: (a) BF-TEM image, and (b) corresponding SADP of a typical region of the UFG layer in A182 induced by the STI machining process (T-S plane).

Summary

- The industrial machining treatment resulted in an outer UFG layer and a subsurface deformed zone in both alloys.
- The extent of the UFG layer and the dimension of the nano-scale grains were strongly affected by the machining processes.
- The presence of large Cu/O particles on the surface of the SAM2 CW 316L specimens may affect the EAC behaviour.
- The effect of machining-induced near-surface deformation is currently being examined in the MEACTOS test program.

References
1. X. Zhong *et al.*, Corrosion Science 115 (2017) pp 106-117, https://doi.org/10.1016/j.corsci.2016.11.019.
2. L. Chang *et al.*, Acta Materialia, 165 (2019), pp 203-214, https://doi.org/10.1016/j.actamat.2018.11.046.
3. A. Maurotto *et al.*, International Journal of Pressure Vessels and Piping, 151 (2017) pp 35-44, https://doi.org/10.1016/j.ijpvp.2017.02.004.

This project receives funding from the Euratom research and training programme 2014-2018 under grant agreement no. 755151.